Enhancement of hepatic autophagy increases ureagenesis and protects against hyperammonemia

Leandro R. Soria[a], Gabriella Allegri[b], Dominique Melck[c], Nunzia Pastore[d,e], Patrizia Annunziata[a], Debora Paris[c], Elena Polishchuk[a], Edoardo Nusco[a], Beat Thöny[b], Andrea Motta[c], Johannes Häberle[b], Andrea Ballabio[a,d,e,f], and Nicola Brunetti-Pierri[a,f,1]

[a]Telethon Institute of Genetics and Medicine, 80078 Pozzuoli, Italy; [b]Division of Metabolism, University Children's Hospital Zurich and Children's Research Center, 8032 Zurich, Switzerland; [c]Institute of Biomolecular Chemistry, National Research Council, 80078 Pozzuoli, Italy; [d]Department of Molecular and Human Genetics, Baylor College of Medicine, Houston, TX 77030; [e]Jan and Dan Duncan Neurological Research Institute, Texas Children's Hospital, Houston, TX 77030; and [f]Department of Translational Medicine, Federico II University, 80131 Naples, Italy

Edited by David W. Russell, University of Texas Southwestern Medical Center, Dallas, TX, and approved November 29, 2017 (received for review August 21, 2017)

Ammonia is a potent neurotoxin that is detoxified mainly by the urea cycle in the liver. Hyperammonemia is a common complication of a wide variety of both inherited and acquired liver diseases. If not treated early and thoroughly, it results in encephalopathy and death. Here, we found that hepatic autophagy is critically involved in systemic ammonia homeostasis by providing key urea-cycle intermediates and ATP. Hepatic autophagy is triggered in vivo by hyperammonemia through an α-ketoglutarate–dependent inhibition of the mammalian target of rapamycin complex 1, and deficiency of autophagy impairs ammonia detoxification. In contrast, autophagy enhancement by means of hepatic gene transfer of the master regulator of autophagy transcription factor EB or treatments with the autophagy enhancers rapamycin and Tat-Beclin-1 increased ureagenesis and protected against hyperammonemia in a variety of acute and chronic hyperammonemia animal models, including acute liver failure and ornithine transcarbamylase deficiency, the most frequent urea-cycle disorder. In conclusion, hepatic autophagy is an important mechanism for ammonia detoxification because of its support of urea synthesis, and its enhancement has potential for therapy of both primary and secondary causes of hyperammonemia.

autophagy | mTORC1 | ornithine transcarbamylase deficiency | hyperammonemia | ureagenesis

Hepatic ureagenesis and glutamine synthesis are the main pathways for waste nitrogen removal in mammals (1, 2). Ammonia crosses the blood–brain barrier and is neurotoxic at high concentration. If left untreated, hyperammonemia can cause irreversible neuronal damage, coma, elevation of intracranial pressure with brain-stem herniation, and death (3). Systemic ammonia is increased in patients with inherited or acquired impairments of ammonia detoxification, such as urea-cycle disorders, organic acidemias, or acute and chronic liver diseases. Current treatments for hyperammonemia are often inadequate (4, 5).

It was previously found that autophagy is induced by ammonia in cultured cancer cells (6, 7). Autophagy is a highly conserved recycling process that degrades cytoplasmic components and organelles in the lysosome (8). It is important in cell homeostasis, and it plays a crucial role in response to a variety of stress conditions, such as nutrient or growth factor limitation, oxidative stress, and accumulation of damaged organelles (9). Among several functions, autophagy monitors and regulates cellular metabolism in the liver (10). Autophagic degradation generates amino acids, free fatty acids, and carbohydrates that can be recycled for synthesis of new cellular components or further oxidized to generate ATP. Autophagy also regulates the cellular energetic balance through the fine-tuned modulation of the number and quality of hepatic mitochondria (11). The mammalian target of rapamycin complex 1 (mTORC1) is a master regulator of cell growth and metabolism and a major signaling pathway regulating autophagy. mTORC1 is a negative regulator of cell catabolism and its inhibition potently induces autophagy (12). Increased autophagy was previously found in the skeletal muscle of mice with hyperammonemia and may contribute to sarcopenia in cirrhosis (13). Nevertheless, the role of ammonia-induced autophagy in liver has not been evaluated so far. In this study, we investigated the role of hepatic autophagy in ammonia detoxification.

Results

Acute Hyperammonemia Activates Hepatic Autophagy. To interrogate the relevance of liver autophagy during hyperammonemia, we used an established in vivo mouse model of acute hyperammonemia (14) in which acute and transient elevations of blood and hepatic ammonia and urea and increased blood glutamine are induced by i.p. injections of 10 mmol/kg of ammonium chloride in C57BL/6 wild-type (WT) mice (*SI Appendix*, Fig. S1 *A–E*). Livers harvested at 0.5 and 2.0 h postammonia challenge showed an increased conversion of LC3I to the autophagosome-associated lipidated form LC3II and reduced levels of two main autophagy substrates (p62/SQSTM1 and NBR1) (Fig. 1 *A* and *B*). In GFP-LC3 transgenic mice (15), i.p. injections of ammonium chloride increased hepatic GFP-LC3 puncta (Fig. 1*C*). By electron microscopy (EM), compared with saline-injected controls, livers of WT mice injected with ammonium chloride showed an increased number of autophagolysosomes (AP/AL) that was similar to control mice injected with Tat-Beclin-1, an autophagy

Significance

Waste nitrogen is converted into urea by the healthy liver. Systemic ammonia is elevated in patients with inherited urea-cycle disorders or acute and chronic liver diseases. Hyperammonemia is a challenging medical condition that holds high risks of mortality and irreversible brain damage. Current treatments are often inadequate. Autophagy is a lysosomal recycling pathway that plays a major role in metabolism. Here, we found that liver autophagy is involved in ammonia homeostasis in vivo and that enhancement of hepatic autophagy increases ureagenesis by providing key urea-cycle intermediates and ATP. Importantly, pharmacological enhancement of autophagy protects against hyperammonemia resulting from both inherited and acquired causes. These findings may lead to development of new drugs promoting ammonia clearance in patients with hyperammonemia.

Author contributions: L.R.S. and N.B.-P. designed research; L.R.S., G.A., D.M., N.P., P.A., E.P., and E.N. performed research; L.R.S., D.M., D.P., B.T., A.M., J.H., A.B., and N.B.-P. analyzed data; and L.R.S. and N.B.-P. wrote the paper.

The authors declare no conflict of interest.

This article is a PNAS Direct Submission.

[1]To whom correspondence should be addressed. Email: brunetti@tigem.it.

This article contains supporting information online at www.pnas.org/lookup/suppl/doi:10.1073/pnas.1714670115/-/DCSupplemental.

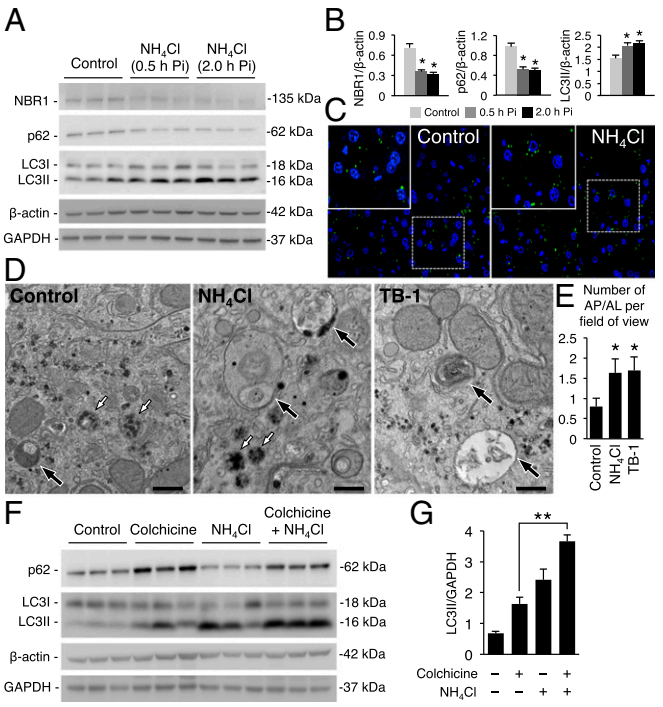

Fig. 1. Acute hyperammonemia activates autophagy in liver. (*A* and *B*) Western blots and densitometric quantifications of NBR1, p62, and LC3 of WT mice with acute hyperammonemia ($n = 3$/group). (*C*) Representative images of GFP-LC3 puncta (autophagosomes) in livers harvested 0.5 h after the injection of either sodium chloride (Control) or ammonium chloride (NH_4Cl) (Magnifications: 63×.) *Insets* show higher magnification of selected areas. (*D*) Representative EM images of livers of mice injected with vehicle (Control), NH_4Cl, or Tat-Beclin-1 (TB-1) and harvested 2.0 h postinjection (Pi). White arrows indicate lysosomes and black arrows indicate AP/AL. (Scale bars, 500 nm.) (*E*) Quantification of AP/AL. (*F*) Inhibition of autophagosome and lysosome fusion by colchicine (0.4 mg/kg i.p. for 3 d) further increased the levels of LC3II and prevented p62 consumption induced by hyperammonemia at 2.0 h after NH_4Cl challenge. (*G*) Densitometric quantifications for LC3II ($n = 3$/group). β-Actin and GAPDH were used as loading controls. $*P < 0.05$; $**P < 0.01$.

inducer peptide (16) (Fig. 1 *D* and *E*). The ammonia challenge was not associated with changes in lysosomal morphology (Fig. 1*D*) and size by EM (lysosomal diameter in controls: 362.5 ± 16.5 nm vs. mice receiving ammonium chloride: 386.4 ± 27.1 nm; $P = 0.47$, unpaired t test). Lysosomal function was also unaffected by hyperammonemia as shown by unchanged hepatic activity of cathepsin B in contrast to livers of control mice injected with the lysosomal inhibitor chloroquine that reduced cathepsin B activity and increased LC3II levels (*SI Appendix*, Fig. S1 *F* and *G*). Increased autophagy flux during hyperammonemia was confirmed in mice treated with colchicine, an inhibitor of microtubule-mediated delivery of autophagosome to lysosome (17) that further increased LC3II and prevented p62 consumption induced by hyperammonemia (Fig. 1 *F* and *G*). Taken together, these results support the activation of hepatic autophagy flux by hyperammonemia in vivo.

Hyperammonemia Induces Hepatic Autophagy Through α-Ketoglutarate-Dependent Inhibition of mTORC1. mTORC1 negatively regulates autophagy by reducing the unc-51–like kinase 1 (ULK1) autophagy initiation complex activity through ULK1 phosphorylation at serine 757 (18). mTORC1 activation was reduced in livers of mice with hyperammonemia, as shown by decreased phosphorylation of P70S6K, ribosomal protein S6, and ULK1 (Fig. 2 *A* and *B*). Active mTORC1 is located on the lysosome surface (12, 19), and consistent with its inhibition, the amount of mTOR in lysosomal fractions from livers of mice with hyperammonemia was reduced compared with controls (Fig. 2 *C* and *D*). Notably, phosphorylation of other kinases regulating autophagy, including AMP-dependent protein kinase (AMPK), extracellular signal-regulated kinase (ERK), and protein kinase B/AKT were unaffected in livers of mice with hyperammonemia (Fig. 2 *A* and *B* and *SI Appendix*, Fig. S2). mTORC1 activity is regulated by various signals including growth factors, cellular stresses, and energy and nutrient levels (12, 19). Activation of mTORC1 and thus autophagy inhibition was found to correlate directly to intracellular concentrations of α-ketoglutarate (α-KG) (20). Consistent with α-KG amination and consequent consumption during hyperammonemia (21–23), hepatic levels of α-KG were reduced during acute hyperammonemia (Fig. 2*E*). Moreover, in vivo supplementation of the cell-permeable α-KG analog dimethyl-α-ketoglutarate (DMKG) (24) rescued α-KG levels and mTORC1 activity (Fig. 2 *E*–*G*). Restoring α-KG levels also prevented ammonia-induced LC3 lipidation (Fig. 2 *H* and *I*) and p62 consumption (*SI Appendix*, Fig. S3), supporting the α-KG–dependent inhibition of hepatic mTORC1 activity during hyperammonemia. Next, we investigated autophagy in livers from WT mice with chronic hyperammonemia induced by a standard diet supplemented with ammonium acetate (20% wt/wt) for 14 wk (25)

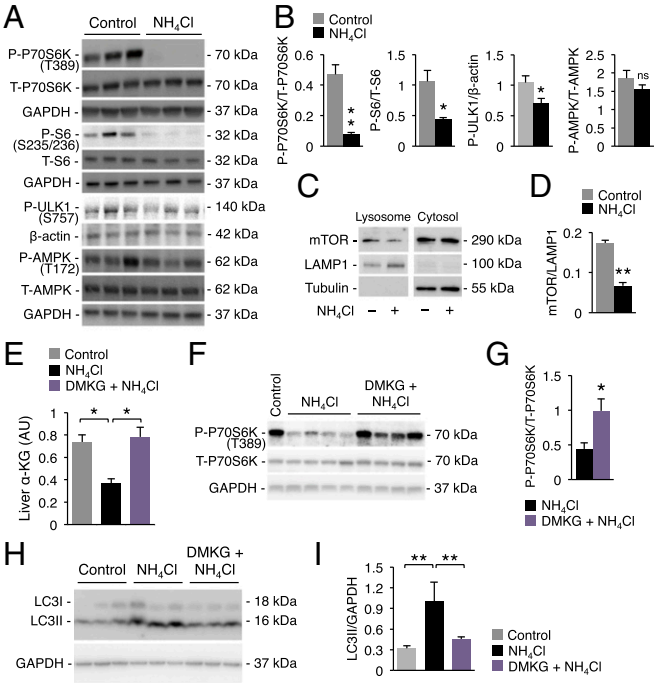

Fig. 2. Acute hyperammonemia induces hepatic autophagy through mTORC1 inhibition as a consequence of reduced hepatic alpha-ketoglutarate. (*A* and *B*) Western blot analyses and densitometric quantifications of phospho (P)-P70S6K, total (T)-P70S6K, P-S6, T-S6, P-ULK1, P-AMPK, and T-AMPK in livers from control and ammonia-treated mice harvested at 0.5 h Pi ($n \geq 3$/group). (*C*) Representative Western blots for mTOR, LAMP1, and Tubulin in the membrane (lysosomes) and cytosol fractions purified from livers of control and NH_4Cl-treated mice at 0.5 h Pi. Samples were run on the same gel but were noncontiguous (*SI Appendix*, Fig. S15). (*D*) Quantification of the mTOR/LAMP1 ratio ($n = 3$/group). (*E*) The α-KG in livers harvested 0.5 h after the injections of saline (control) or NH_4Cl in mice treated with DMKG (500 mg/kg i.p. for 3 d and 1 h before the ammonia i.p. injections) or vehicle. (*F* and *G*) Western blot analyses and densitometric quantifications of P-P70S6K and T-P70S6K in livers from DMKG-treated ($n = 6$) and vehicle-treated mice ($n = 4$) harvested at 0.5 h post NH_4Cl injection. A control sample of liver from a mouse treated with vehicle but not with NH_4Cl is also shown. (*H* and *I*) Representative Western blotting and densitometric quantifications of LC3 in livers of mice treated with vehicle, NH_4Cl, or DMKG plus NH_4Cl. Control: $n = 4$; NH_4Cl: $n = 4$; DMKG + NH_4Cl: $n = 6$. GAPDH or β-actin were used as loading controls. $*P < 0.05$; $**P < 0.01$. ns, not significant.

that increased serum urea whereas serum glutamine was unaffected (*SI Appendix*, Fig. S4 *A* and *B*). Livers of mice with chronic hyperammonemia showed increased hepatic autophagy, as indicated by reduced substrates (NBR1 and p62) and increased LC3II levels (Fig. 3 *A* and *B*). Moreover, chronic hyperammonemia was associated with reduced activation of mTORC1 as shown by decreased phosphorylation of S6 and ULK1 and reduced intrahepatic levels of α-KG without effects on AMPK signaling, similar to the acute hyperammonemia (Fig. 3 *C* and *D* and *SI Appendix*, Fig. S4 *C*, *D*, and *E*). mTOR also regulates autophagy by phosphorylation affecting nuclear translocation of the transcription factor EB (TFEB), a master regulator of autophagy and lysosomal function (26, 27). Notably, despite reduced mTORC1 activity, both the nuclear localization of TFEB and the expression of its target genes were not increased in livers of mice with acute or chronic hyperammonemia (*SI Appendix*, Fig. S5). Taken together, these data support in vivo hepatic activation of autophagy by both acute and chronic hyperammonemia through mTORC1 inhibition as a consequence of intrahepatic α-KG depletion.

Hepatic Autophagy Is Important for Ammonia Detoxification. To investigate the role of autophagy in ammonia detoxification, we measured blood ammonia levels during acute hyperammonemia in mice with defective autophagy. We knocked-down *Atg7* in hepatocytes of mice carrying the *Atg7* floxed allele ($Atg7^{fl/fl}$) (28) by i.v. injections of a helper-dependent adenoviral (HDAd) vector expressing Cre under the control of a liver-specific expression cassette (HDAd-Cre) (29). In these mice, an ∼50% knockdown of hepatic *Atg7* impairing autophagy as shown by increased p62 and LC3II (Fig. 4 *A* and *B*) resulted in higher levels of serum ammonia after ammonium chloride challenge compared with control $Atg7^{fl/fl}$ mice injected with a HDAd vector encoding the unrelated, nontoxic, nonimmunogenic alpha-fetoprotein reporter gene under the control of the same liver-specific expression cassette (HDAd-AFP) (29) (Fig. 4*C*). Consistently, in vivo hepatic loss- or gain-of-function of TFEB resulted in defective or enhanced ammonia detoxification, respectively. Higher levels of ammonia were indeed detected postammonium chloride challenge in mice with hepatic deletion of TFEB (30) compared with

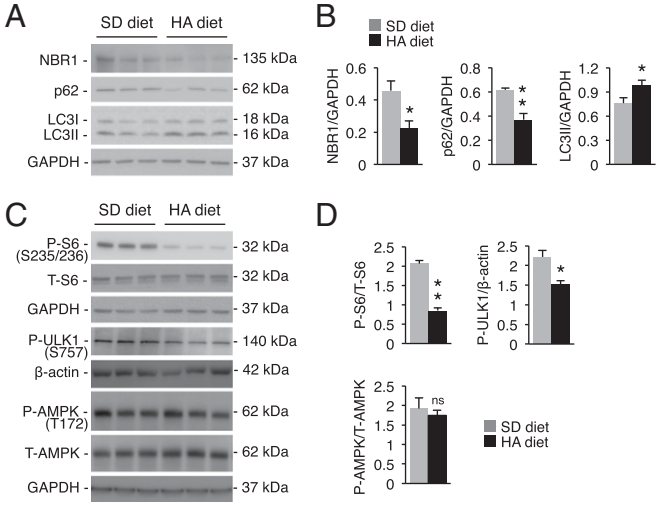

Fig. 3. Chronic hyperammonemia activates hepatic autophagy through mTORC1 inhibition. (*A* and *B*) Western blots and densitometric quantifications of NBR1, p62, and LC3 in livers of WT mice fed for 14 wk with a diet containing ammonium acetate (HA diet) or with a standard diet (SD diet) (n = 3/group). (*C* and *D*) Western blot analyses and densitometric quantifications of phospho (P)-S6, total (T)-S6, P-ULK1, P-AMPK, and T-AMPK in livers of WT that received either SD diet or HA diet for 14 wk resulting in chronic hyperammonemia ($n \geq 3$/group). GAPDH or β-actin were used as loading controls. $^*P < 0.05$; $^{**}P < 0.01$. ns, not significant.

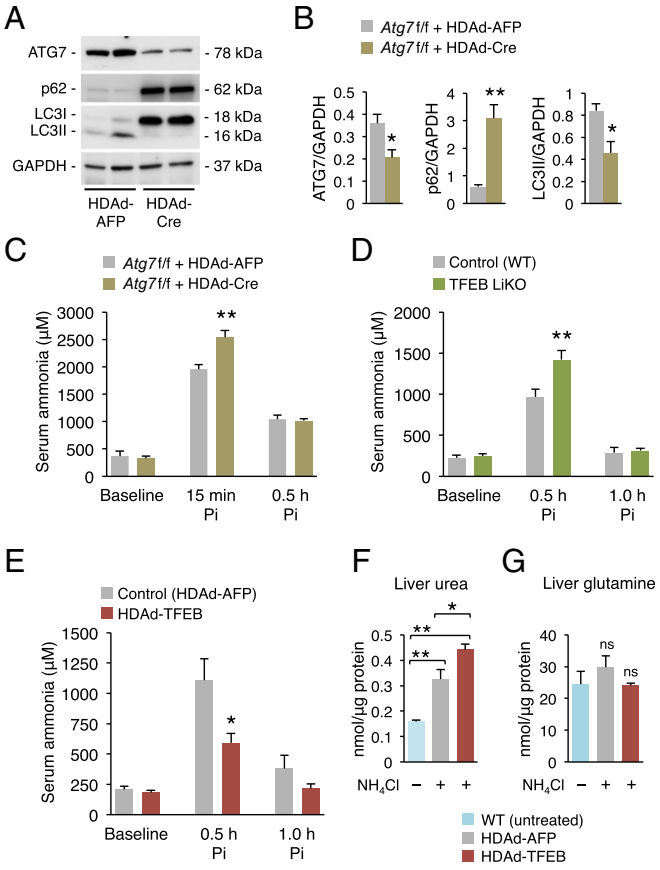

Fig. 4. Hepatic autophagy is important for ammonia detoxification. (*A* and *B*) Representative bands and densitometric quantifications of Western blotting of ATG7, p62, and LC3 of livers harvested at 1.0 h post-NH_4Cl injection from $Atg7^{fl/fl}$ mice injected with HDAd-Cre or with a control vector (HDAd-AFP) 4 wk before the ammonia challenge ($n \geq 3$/group). GAPDH was used as loading control. (*C*) Serum ammonia at baseline, 15 min and 0.5 h after i.p. injections of NH_4Cl in $Atg7^{fl/fl}$ mice injected with HDAd-Cre (n = 5) or HDAd-AFP vector (n = 4). (*D*) Serum ammonia in WT (Control, n = 12) and TFEB liver-specific knockout mice (TFEB LiKO, n = 13) at baseline, 0.5 and 1.0 h after i.p. injections of NH_4Cl. (*E*) Serum ammonia in WT mice injected with HDAd-TFEB or HDAd-AFP vector (n = 5/group) at baseline, 0.5 and 1.0 h after i.p. injections of NH_4Cl. (*F* and *G*) Urea and glutamine in livers harvested at 2.0 h post-NH_4Cl injection in WT mice injected with HDAd-AFP or HDAd-TFEB (n = 5/group). Control untreated WT mice are included (n = 3). $^*P < 0.05$; $^{**}P < 0.01$. ns, not significant.

WT controls (Fig. 4*D*). Conversely, hepatic gene transfer of the human TFEB in WT mice mediated by HDAd vectors (HDAd-TFEB) (31) (*SI Appendix*, Fig. S6*A*) resulted in increased autophagy in livers as shown by reduced hepatic p62 and increased LC3II (*SI Appendix*, Fig. S6 *B* and *C*), reduced blood ammonia, and increased hepatic urea content compared with control mice injected with the HDAd-AFP vector (Fig. 4 *E* and *F*), whereas liver glutamine was not increased (Fig. 4*G*). The reduced blood ammonia levels were not dependent on increased expression of the urea-cycle enzymes that were unchanged in HDAd-TFEB–injected mice compared with controls (*SI Appendix*, Fig. S7). Taken together, these results suggest that hepatic autophagy during hyperammonemia cooperates with the urea cycle for efficient ammonia detoxification.

Hepatic Autophagy Increases Ureagenesis by Providing Key Urea-Cycle Intermediates. To demonstrate that autophagy activation was associated with increased ureagenesis, we administered ^{15}N-labeled ammonium chloride to WT mice treated with Tat-Beclin-1 or vehicle and analyzed blood by ^{15}N-NMR. Administration of

MEDICAL SCIENCES

Tat-Beclin-1 (20 mg/kg i.p.) 2 h before the ammonium chloride challenge increased autophagy in livers, as shown by reduced hepatic p62 and increased LC3II (*SI Appendix*, Fig. S8), and resulted in increased ureagenesis and improved ammonia clearance, as shown by markedly increased blood levels of ^{15}N-labeled urea (Fig. 5*A*) and reduced concentration of blood ammonia (Fig. 5*B*), respectively. Moreover, high-resolution ^{1}H-NMR spectroscopy showed that the whole-liver metabolome of mice with hyperammonemia was well separated from controls, but it was shifted toward the nonhyperammonemia controls in mice injected with Tat-Beclin-1 (Fig. 5*C* and *SI Appendix*, Fig. S9). Interestingly, by metabolite set enrichment analysis, pathways altered between hyperammonemic livers and controls and between hyperammonemic livers of mice treated with Tat-Beclin-1 or vehicle were largely overlapping (*SI Appendix*, Fig. S10). Taken together, these findings suggest that autophagy stimulation rescued the metabolic changes induced by hyperammonemia at least partially. Next, we evaluated the levels of intermediate substrates and metabolites essential for the functioning of the urea cycle. Higher levels of ATP, aspartate, acetyl-coA, and glutamate were detected in livers after the ammonia challenge in WT mice injected with Tat-Beclin-1 compared with vehicle-treated controls, whereas acetyl-coA and glutamate also were increased by Tat-Beclin-1 at baseline (Fig. 5 *D*–*G*). The urea cycle requires induction by *N*-acetylglutamate (NAG), the allosteric activator of carbamoylphosphate synthetase 1 (CPS1) that catalyzes the first step of the cycle (32). In addition to NAG, which is synthesized from acetyl-coA and glutamate, ureagenesis also requires ATP and aspartate to fuel the urea cycle.

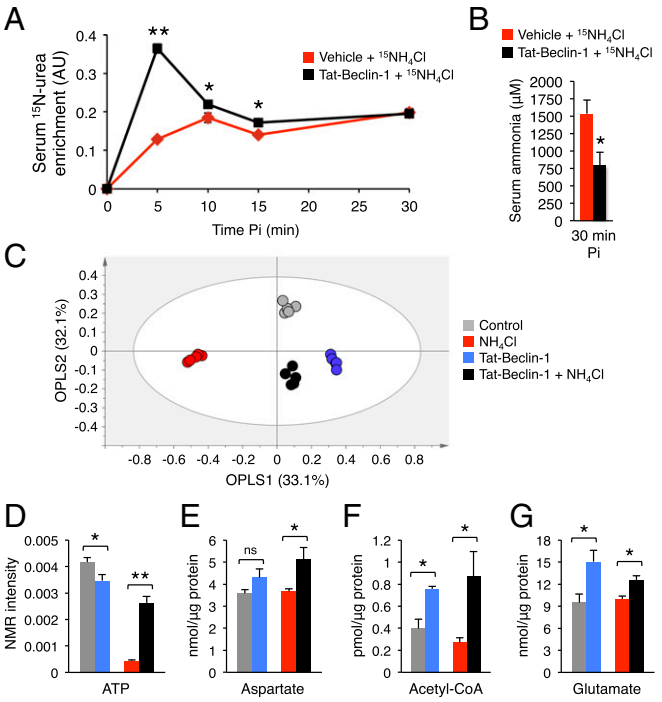

Fig. 5. Hepatic autophagy increases ureagenesis by providing key urea-cycle intermediates. (*A*) Serum levels of ^{15}N-labeled urea after i.p. injection of $^{15}NH_4Cl$ in vehicle and Tat-Beclin-1 (20 mg/kg i.p. 2 h before $^{15}NH_4Cl$ administration) treated WT mice ($n \geq 4$/group). (*B*) Serum ammonia at 30 min after i.p. injection of $^{15}NH_4Cl$ in vehicle ($n = 6$) and Tat-Beclin-1 ($n = 9$) treated mice. (*C*) Orthogonal Projection to Latent Structure-Discriminant Analysis (OPLS-DA) score plot. A complex, nonoverfitted three predictive components model with $R^2 = 98.2\%$ (goodness of fit) and $Q^2 = 82.7\%$ (power in prediction) with $P = 0.0038$ was obtained ($n = 5$). See also *SI Appendix*, Figs. S9 and S10. (*D*–*G*) ATP, aspartate, acetyl-coA, and glutamate contents in livers from control mice, mice with acute hyperammonemia, Tat-Beclin-1–treated mice without hyperammonemia, and Tat-Beclin-1–treated mice with acute hyperammonemia ($n \geq 3$/group). *$P < 0.05$; **$P < 0.01$. ns, not significant.

During hyperammonemia, increased levels of NAG precursors, ATP, and aspartate induced by autophagy can activate and fuel the urea cycle, thus providing a potential mechanism underlying the improved ammonia detoxification in livers with autophagy enhancement.

Enhancement of Hepatic Autophagy Protects Against Acute and Chronic Hyperammonemia. Next, we investigated the efficacy of autophagy inducers, namely rapamycin and Tat-Beclin-1 for therapy of acute hyperammonemia. Rapamycin (2 mg/kg i.p. for 3 d) resulted in increased hepatic autophagy (*SI Appendix*, Fig. S11) and protection against acute hyperammonemia in WT mice compared with control mice injected with vehicle (Fig. 6*A*). Similar results were obtained with Tat-Beclin-1 (Fig. 6*A*). For both treatments hepatic urea was increased whereas the liver amount of glutamine was unaffected (*SI Appendix*, Fig. S12). Ammonia is converted to urea by the healthy liver but during liver failure, normal ammonia detoxification capacity is impaired and circulating ammonia increases resulting in hepatic encephalopathy and brain dysfunction (33). Mice with mild hepatic failure induced by i.p. administration of thioacetamide develop hyperammonemia (34). Thus, we investigated whether activators of autophagy are effective in protection against hyperammonemia induced by acute liver failure. Mice that received rapamycin or Tat-Beclin-1 showed a significant decrease of blood ammonia levels during acute liver failure induced by thioacetamide (Fig. 6 *B* and *C*). Induction of hepatic autophagy was confirmed by LC3 Western blotting for both treatments (*SI Appendix*, Fig. S13 *A* and *B*). Moreover, serum levels of alanine aminotransferase (ALT), a marker of liver injury, were similar among control vehicle- and drug-treated groups (*SI Appendix*, Fig. S13*C*), suggesting that the effects of rapamycin and Tat-Beclin-1 on reducing blood ammonia were not dependent on decreased liver damage.

Finally, we investigated whether autophagy enhancement protects against chronic hyperammonemia using rapamycin, a drug already used for long-term treatments in humans (35) and thus, with higher potential for clinical translation. WT mice fed an ammonia-enriched diet showed increased blood ammonia, but rapamycin reduced blood ammonia to levels that were similar to control mice fed with a standard diet (Fig. 6*D*). Moreover, rapamycin increased ^{15}N-labeled urea enrichment and normalized orotic acid concentration in whole blood/dried spots (36) of sparse fur, abnormal skin and hair (*spf^{ash}*) mice, a model of constitutive hyperammonemia due to marked reduction (about 5% of normal activity) of the ornithine transcarbamylase (OTC) activity (37) (Fig. 6 *E* and *F*). As expected, rapamycin-injected *spf^{ash}* mice showed decreased phosphorylation of ribosomal protein S6 (*SI Appendix*, Fig. S14 *A* and *B*). Of note, rescue of *spf^{ash}* biochemical correction was not dependent on increased OTC activity that was unaffected by rapamycin treatment (*SI Appendix*, Fig. S14*C*). Together, these results suggest that pharmacological enhancement of autophagy is effective for therapy of acute and chronic hyperammonemia occurring in both acquired and genetic disorders.

Discussion

Hyperammonemia is a consequence of defects in the metabolism of waste nitrogen from breakdown of proteins and other nitrogen-containing molecules such as nucleic acids. Survival in patients with hyperammonemia closely correlates with the levels of blood ammonia and improves by treatments lowering ammonia (38). Our study suggests the concept that autophagy potentiates ureagenesis under both acute and chronic hyperammonemia. Importantly, this study provides pharmacologic approaches for therapy of a common debilitating and life-threatening complication of a wide range of liver diseases.

The previously published studies in cell models showed that ammonia has a dual effect on autophagy: activation at low concentrations and inhibition at higher concentrations (6, 7, 39, 40). Moreover, the mechanism by which ammonia induces autophagy remains controversial. It was initially reported that

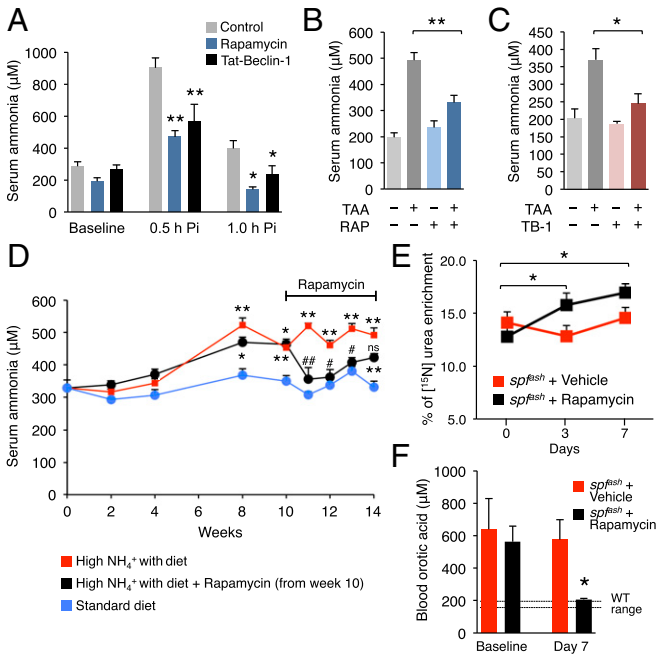

Fig. 6. Enhancement of hepatic autophagy protects against acute and chronic hyperammonemia. (*A*) Serum ammonia at baseline, 0.5 and 1.0 h after i.p. injection of NH_4Cl in WT mice ($n \geq 5$/group) treated with vehicle (control), rapamycin (2 mg/kg i.p. for 3 d), or Tat-Beclin-1 (20 mg/kg i.p. for 2 h). (*B* and *C*) Pharmacological enhancement of autophagy by rapamycin (Rap) (2 mg/kg for 3 d i.p., $n \geq 9$) or Tat-Beclin-1 (TB-1) (15 mg/kg for 3 d i.p., $n \geq 4$) protects against acute hyperammonemia during thioacetamide-induced liver failure. TAA, thioacetamide (250 mg/kg i.p. 24 h before sacrifice). (*D*) Serum ammonia levels in WT mice fed with a standard diet or with a standard diet supplemented with ammonium acetate (20% wt/wt). Rapamycin (2 mg/kg every 48 h, i.p.) or vehicle was started at 10 wk and continued up to 14 wk in mice fed with the diet supplemented with ammonium acetate ($n \geq 8$/group). (*E*) Isotopic enrichment of ^{15}N-labeled urea measured in whole blood/dried blood spots, 30 min after i.p. injection of $^{15}NH_4Cl$ tracer (4 mmol/kg) in spf^{ash} mice treated with rapamycin (10 mg/kg/d i.p.) at baseline, 3 d and 7 d compared with vehicle-treated mice ($n \geq 4$/group). (*F*) Orotic acid was determined in whole blood/dried blood spots in spf^{ash} mice at day 0 (baseline) and day 7 of rapamycin or vehicle treatment ($n \geq 4$/group). In *D*: *statistically significant vs. standard diet, #statistically significant vs. high-ammonia diet. $^{*,\#}P < 0.05$; $^{**,\#\#}P < 0.01$. ns, not significant.

ammonia-induced autophagy was independent of mTORC1 (6, 7). However, subsequent studies found ammonia-induced changes in the mTORC1 pathway including both inhibition and activation (41–43). This likely reflects context and dose-dependent interactions between ammonia and mTORC1. In this study, we found that liver autophagy is triggered by hyperammonemia through inhibition of mTORC1. These data are in line with previous studies that associated hyperammonemia with increased autophagy (13) and inhibition of mTORC1 signaling in skeletal muscle (44, 45). Hepatic AMPK signaling has been linked to ureagenesis during conditions of increased amino acid flux (46). However, AMPK activation in livers was unaffected by elevated ammonia, thus reflecting differential pathway activation in response to ammonia or amino acids.

mTORC1 activity is regulated by several metabolic signals, including the tricarboxylic acid cycle intermediate α-KG (20, 24). Activation of mTORC1 directly correlates with intracellular concentrations of α-KG, which promote translocation of mTORC1 to the lysosome surface and its activation (20). Here, we show that hepatic mTORC1 inhibition during hyperammonemia is dependent on α-KG levels. Reduced hepatic levels of α-KG during acute ammonia overload are consistent with its function as nitrogen scavenger and as a source of aspartate and NAG (21–23). Supplementations in vivo with an α-KG analog that rescued mTORC1 activity and prevented ammonia-induced autophagy provide robust evidence for an α-KG–dependent modulation of hepatic mTORC1 activity during hyperammonemia. Hence, our data are consistent with previous studies showing a direct correlation between α-KG levels and mTORC1 activity (20, 24, 47–49). The activity of the oxygen sensors EGLN/prolyl hydroxylases that require oxygen and α-KG for hydroxylation of target proteins has been proposed to explain α-KG–dependent activation of mTORC1 (48). Further studies are required to establish whether EGLNs/prolyl hydroxylases are involved in activation of autophagy during hyperammonemia.

During hyperammonemia to keep pace with the rapid incorporation of ammonia into mitochondrial CPS1, hepatic proteolysis is induced to provide aspartate to form argininosuccinate that fuels the urea cycle and promotes ammonia clearance (50). In line with this, previous studies showed that delivery of urea-cycle intermediates prevented ammonia toxicity after an acute nitrogen load in both WT and spf^{ash} mice (51, 52). In this study, we found that ammonia detoxification capacity in mice with suppressed autophagy was impaired, suggesting that the liver requires a functional autophagic pathway for efficient ammonia detoxification. Moreover, autophagy enhancement by hepatic gene transfer of TFEB or administration of small molecules (rapamycin or Tat-Beclin-1) increased ureagenesis and protected against hyperammonemia in a variety of models of acute and chronic liver diseases, including the spf^{ash} mouse. Studies with a stable isotope to evaluate metabolic flux and liver metabolomic analyses suggested that during hyperammonemia autophagy potentiates ureagenesis by furnishing the urea cycle with key intermediate metabolites (aspartate and NAG precursors) and by preventing ammonia-induced depletion of ATP. In addition to periportal ureagenesis, ammonia is efficiently cleared in perivenous hepatocytes by glutamine synthetase (53, 54). Moreover, disposal of glutamine-bound ammonia to urea was recently found to depend on the rate of glutamine synthesis (54). Although we did not detect an increase in glutamine levels, we cannot rule out a contribution of hepatic glutamine synthesis during the autophagy-induced improvement in ammonia detoxification.

Available therapeutic options to treat hyperammonemia are often unsatisfactory because of limited efficacy, side effects, and elevated costs. Therefore, the development of novel therapies for hyperammonemia is highly needed (55). Here, we have found that pharmacological enhancement of autophagy may be an effective therapeutic strategy for acute and chronic hyperammonemia of acquired and genetic disorders. In our proof-of-principle experiments, we focused on rapamycin, a drug already used for long-term treatments in humans (35, 56). However, several Food and Drug Administration-approved drugs are known inducers of autophagy and might be investigated for hyperammonemia therapy. Nevertheless, target specificity and potential undesired side effects have to be taken into account for the choice of the optimal autophagy enhancer for hyperammonemia therapy (56). In addition, combinatorial treatments based on drugs enhancing ammonia excretion, urea synthesis, and hepatic autophagy could cooperate for more efficient ammonia detoxification. In conclusion, our data show that hepatic autophagy is an important mechanism for ammonia detoxification and that its enhancement can be exploited therapeutically for both acute and chronic hyperammonemia occurring in acquired hepatic diseases and inherited disorders of the urea cycle.

Materials and Methods

Mouse Procedures. Mouse procedures were performed in accordance with regulations of the Animal Care and Use Committee of Cardarelli Hospital in Naples and were authorized by the Italian Ministry of Health, and the Veterinary Office of the State of Zurich and Swiss law on animal protection, the Swiss Federal Act on Animal Protection (1978), and the Swiss Animal Protection Ordinance (1981). Male 6-wk-old C57BL/6 (Charles River Laboratories), transgenic GFP-LC3 (15), *Atg7* floxed allele ($Atg7^{fl/fl}$) (28), TFEB liver-specific knockout (TFEB LiKO) (30), and Otc-sparse fur, abnormal skin and hair (spf^{ash}) (36) mice were used and were randomly assigned to treatment groups.

Investigators were not blinded to allocation during experiments and outcome assessment. See *SI Appendix, SI Material and Methods* for detailed descriptions of mouse and methodological procedures.

Statistical Analyses. Data are expressed as means ± SEM. A two-tailed paired Student's *t* test was performed when comparing the same group of mice at two different time points. A two-tailed unpaired Student's *t* test was performed when comparing two groups of mice. One-way ANOVA and Tukey's post hoc tests were performed when comparing more than two groups relative to a single factor. Two-way ANOVA and Tukey's post hoc tests were performed when comparing more than two groups relative to two factors. NMR data statistical analyses are detailed in *SI Appendix, SI Material and Methods*. No statistical methods were used to predetermine the sample size. A P value < 0.05 was considered statistically significant.

ACKNOWLEDGMENTS. We thank A. Carissimo from the Telethon Institute of Genetics and Medicine Bioinformatics Core for assistance with statistical analyses and C. Settembre and G. Diez-Roux for critical reading of the manuscript. L.R.S. was supported by the Dulbecco Telethon Institute International Mobility for Postdoctoral Research Training (DTI-IMPORT) Marie Skłodowska-Curie COFUND program. G.A. was supported by Roche Pharma. This work was supported by the European Research Council (IEMTx) (N.B.-P.) and Fondazione Telethon Italy Grants TCBP37TELC and TCBMT3TELD (to N.B.-P.).

1. Meijer AJ, Lamers WH, Chamuleau RA (1990) Nitrogen metabolism and ornithine cycle function. *Physiol Rev* 70:701–748.
2. Haüssinger D (1990) Nitrogen metabolism in liver: Structural and functional organization and physiological relevance. *Biochem J* 267:281–290.
3. Lee WM, Squires RH, Jr, Nyberg SL, Doo E, Hoofnagle JH (2008) Acute liver failure: Summary of a workshop. *Hepatology* 47:1401–1415.
4. Häberle J (2013) Clinical and biochemical aspects of primary and secondary hyperammonemic disorders. *Arch Biochem Biophys* 536:101–108.
5. Riordan SM, Williams R (1997) Treatment of hepatic encephalopathy. *N Engl J Med* 337:473–479.
6. Eng CH, Yu K, Lucas J, White E, Abraham RT (2010) Ammonia derived from glutaminolysis is a diffusible regulator of autophagy. *Sci Signal* 3:ra31.
7. Cheong H, Lindsten T, Wu J, Lu C, Thompson CB (2011) Ammonia-induced autophagy is independent of ULK1/ULK2 kinases. *Proc Natl Acad Sci USA* 108:11121–11126.
8. Mizushima N, Komatsu M (2011) Autophagy: Renovation of cells and tissues. *Cell* 147:728–741.
9. Rabinowitz JD, White E (2010) Autophagy and metabolism. *Science* 330:1344–1348.
10. Ueno T, Komatsu M (2017) Autophagy in the liver: Functions in health and disease. *Nat Rev Gastroenterol Hepatol* 14:170–184.
11. Madrigal-Matute J, Cuervo AM (2016) Regulation of liver metabolism by autophagy. *Gastroenterology* 150:328–339.
12. Saxton RA, Sabatini DM (2017) mTOR signaling in growth, metabolism, and disease. *Cell* 168:960–976.
13. Qiu J, et al. (2012) Hyperammonemia-mediated autophagy in skeletal muscle contributes to sarcopenia of cirrhosis. *Am J Physiol Endocrinol Metab* 303:E983–E993.
14. Ye X, et al. (1997) Adenovirus-mediated in vivo gene transfer rapidly protects ornithine transcarbamylase-deficient mice from an ammonium challenge. *Pediatr Res* 41:527–534.
15. Mizushima N, Yamamoto A, Matsui M, Yoshimori T, Ohsumi Y (2004) In vivo analysis of autophagy in response to nutrient starvation using transgenic mice expressing a fluorescent autophagosome marker. *Mol Biol Cell* 15:1101–1111.
16. Shoji-Kawata S, et al. (2013) Identification of a candidate therapeutic autophagy-inducing peptide. *Nature* 494:201–206.
17. Ju JS, Varadhachary AS, Miller SE, Weihl CC (2010) Quantitation of "autophagic flux" in mature skeletal muscle. *Autophagy* 6:929–935.
18. Kim J, Kundu M, Viollet B, Guan KL (2011) AMPK and mTOR regulate autophagy through direct phosphorylation of Ulk1. *Nat Cell Biol* 13:132–141.
19. Lim CY, Zoncu R (2016) The lysosome as a command-and-control center for cellular metabolism. *J Cell Biol* 214:653–664.
20. Durán RV, et al. (2012) Glutaminolysis activates Rag-mTORC1 signaling. *Mol Cell* 47:349–358.
21. Cooper AJ, Nieves E, Coleman AE, Filc-DeRicco S, Gelbard AS (1987) Short-term metabolic fate of [13N]ammonia in rat liver in vivo. *J Biol Chem* 262:1073–1080.
22. Brosnan JT, Brosnan ME, Charron R, Nissim I (1996) A mass isotopomer study of urea and glutamine synthesis from 15N-labeled ammonia in the perfused rat liver. *J Biol Chem* 271:16199–16207.
23. Nissim I, et al. (2003) Role of the glutamate dehydrogenase reaction in furnishing aspartate nitrogen for urea synthesis: Studies in perfused rat liver with 15N. *Biochem J* 376:179–188.
24. Mariño G, et al. (2014) Regulation of autophagy by cytosolic acetyl-coenzyme A. *Mol Cell* 53:710–725.
25. Azorín I, Miñana MD, Felipo V, Grisolía S (1989) A simple animal model of hyperammonemia. *Hepatology* 10:311–314.
26. Settembre C, et al. (2011) TFEB links autophagy to lysosomal biogenesis. *Science* 332:1429–1433.
27. Settembre C, et al. (2012) A lysosome-to-nucleus signalling mechanism senses and regulates the lysosome via mTOR and TFEB. *EMBO J* 31:1095–1108.
28. Komatsu M, et al. (2005) Impairment of starvation-induced and constitutive autophagy in Atg7-deficient mice. *J Cell Biol* 169:425–434.
29. Brunetti-Pierri N, et al. (2006) Improved hepatic transduction, reduced systemic vector dissemination, and long-term transgene expression by delivering helper-dependent adenoviral vectors into the surgically isolated liver of nonhuman primates. *Hum Gene Ther* 17:391–404.
30. Settembre C, et al. (2013) TFEB controls cellular lipid metabolism through a starvation-induced autoregulatory loop. *Nat Cell Biol* 15:647–658.
31. Pastore N, et al. (2013) Gene transfer of master autophagy regulator TFEB results in clearance of toxic protein and correction of hepatic disease in alpha-1-anti-trypsin deficiency. *EMBO Mol Med* 5:397–412.
32. Morizono H, Caldovic L, Shi D, Tuchman M (2004) Mammalian N-acetylglutamate synthase. *Mol Genet Metab* 81(Suppl 1):S4–S11.
33. Bhatia V, Singh R, Acharya SK (2006) Predictive value of arterial ammonia for complications and outcome in acute liver failure. *Gut* 55:98–104.
34. Nicaise C, et al. (2008) Control of acute, chronic, and constitutive hyperammonemia by wild-type and genetically engineered Lactobacillus plantarum in rodents. *Hepatology* 48:1184–1192.
35. Levine B, Packer M, Codogno P (2015) Development of autophagy inducers in clinical medicine. *J Clin Invest* 125:14–24.
36. Allegri G, et al. (2017) A simple dried blood spot-method for in vivo measurement of ureagenesis by gas chromatography-mass spectrometry using stable isotopes. *Clin Chim Acta* 464:236–243.
37. Hodges PE, Rosenberg LE (1989) The spfash mouse: A missense mutation in the ornithine transcarbamylase gene also causes aberrant mRNA splicing. *Proc Natl Acad Sci USA* 86:4142–4146.
38. Clemmesen JO, Larsen FS, Kondrup J, Hansen BA, Ott P (1999) Cerebral herniation in patients with acute liver failure is correlated with arterial ammonia concentration. *Hepatology* 29:648–653.
39. Seglen PO, Grinde B, Solheim AE (1979) Inhibition of the lysosomal pathway of protein degradation in isolated rat hepatocytes by ammonia, methylamine, chloroquine and leupeptin. *Eur J Biochem* 95:215–225.
40. Polletta L, et al. (2015) SIRT5 regulation of ammonia-induced autophagy and mitophagy. *Autophagy* 11:253–270.
41. Harder LM, Bunkenborg J, Andersen JS (2014) Inducing autophagy: A comparative phosphoproteomic study of the cellular response to ammonia and rapamycin. *Autophagy* 10:339–355.
42. Li Z, et al. (2016) Ammonia induces autophagy through dopamine receptor D3 and MTOR. *PLoS One* 11:e0153526.
43. Merhi A, Delrée P, Marini AM (2017) The metabolic waste ammonium regulates mTORC2 and mTORC1 signaling. *Sci Rep* 7:44602.
44. Davuluri G, et al. (2016) Metabolic adaptation of skeletal muscle to hyperammonemia drives the beneficial effects of l-leucine in cirrhosis. *J Hepatol* 65:929–937.
45. Kumar A, et al. (2017) Ammonia lowering reverses sarcopenia of cirrhosis by restoring skeletal muscle proteostasis. *Hepatology* 65:2045–2058.
46. Madiraju AK, et al. (2016) Argininosuccinate synthetase regulates hepatic AMPK linking protein catabolism and ureagenesis to hepatic lipid metabolism. *Proc Natl Acad Sci USA* 113:E3423–E3430.
47. Xu P, et al. (2016) LRH-1-dependent programming of mitochondrial glutamine processing drives liver cancer. *Genes Dev* 30:1255–1260.
48. Durán RV, et al. (2013) HIF-independent role of prolyl hydroxylases in the cellular response to amino acids. *Oncogene* 32:4549–4556.
49. Yoon WH, et al. (2017) Loss of nardilysin, a mitochondrial co-chaperone for α-ketoglutarate dehydrogenase, promotes mTORC1 activation and neurodegeneration. *Neuron* 93:115–131.
50. Brosnan JT, et al. (2001) Alanine metabolism in the perfused rat liver. Studies with (15)N. *J Biol Chem* 276:31876–31882.
51. Sarhan S, Knoedgen B, Seiler N (1994) Protection against lethal ammonia intoxication: Synergism between endogenous ornithine and L-carnitine. *Metab Brain Dis* 9:67–79.
52. Marini JC, Lee B, Garlick PJ (2006) Ornithine restores ureagenesis capacity and mitigates hyperammonemia in Otc(spf-ash) mice. *J Nutr* 136:1834–1838.
53. Qvartskhava N, et al. (2015) Hyperammonemia in gene-targeted mice lacking functional hepatic glutamine synthetase. *Proc Natl Acad Sci USA* 112:5521–5526.
54. Hakvoort TB, et al. (2017) Pivotal role of glutamine synthetase in ammonia detoxification. *Hepatology* 65:281–293.
55. Matoori S, Leroux JC (2015) Recent advances in the treatment of hyperammonemia. *Adv Drug Deliv Rev* 90:55–68.
56. Galluzzi L, Bravo-San Pedro JM, Levine B, Green DR, Kroemer G (2017) Pharmacological modulation of autophagy: Therapeutic potential and persisting obstacles. *Nat Rev Drug Discov* 16:487–511.